33rd Annual International Conference of the IEEE EMBS
Boston, Massachusetts USA, August 30 - September 3, 2011

Rapid Impedance Measurement of Tethered Bilayer Lipid Membrane Biosensors

Xiaoyi Mu, Daniel Rairigh, Xiaowen Liu, Andrew J. Mason, *Senior Member, IEEE*
Electrical and Computer Engineering, Michigan State Univ., East Lansing, MI, USA

***Abstract*—Tethered bilayer lipid membranes (tBLM) offer a promising means to immobilize membrane proteins for sensor applications and study biological phenomena including membrane-nanoparticle interactions. tBLM biointerfaces are typically characterized using electrochemical impedance spectroscopy (EIS) in the 1mHz to 1Hz range due to interface parasitics. To enable rapid characterization of biointerfaces for high throughput applications, this paper introduces a method for high resolution EIS characterization of tBLMs at higher frequencies. The tBLM equivalent electrical model is analyzed, and the benefit of extracting the real portion of interface admittance is described. Mathematical analysis shows that the maximum frequency for measuring membrane resistance is a function of membrane characteristics and that small area membranes could enable measurement well into the kHz range, permitting observation of millisecond membrane protein activity in biosensor arrays.**

I. Introduction

Because of the critical role membrane proteins play in biological function, biosensors utilizing membrane proteins have become increasingly attractive in bioanalytical and medical applications such as drug screening, medical diagnostics and biophyscial characterization of channels [1, 2]. Characterization of membrane proteins using electrochemical impedance spectroscopy (EIS) facilitates continuous use and label-free sensing with significant advantages over affinity-based sensors [3-6]. Tethered bilayer lipid membranes (tBLM) are artificial biomimetic structures that can immobilize membrane proteins without denaturing and are thus promising for realization of membrane protein arrays. tBLM is also highly useful to study interactions between biomembranes and nanoparticles to better understand nanoparticle toxicity/safety profiles. Electrochemical biosensors featuring tBLMs [7, 8] show great potential as a platform for biochemical sensing and fundamental investigations of biomolecular behavior.

EIS is a widely used technique for label-free characterization of biosensors wherein the sensor's impedance spectrum is fit to an equivalent electrical model. The electrical model parameter values and changes in values over time reveal important biological information such as ion channel activity and bonding mechanisms. Utilizing EIS, measurements of tBLM and similar sensors with sub-second resolution have been realized [9-12]. However, real-time monitoring of single channel activity, important to many applications, requires millisecond response that is not provided by any reported tBLM system.

This paper introduces an EIS-based method for real-time characterization of tBLM membrane protein activity with high resolution. Section II describes the tBLM equivalent electrical model and Section III discusses the pros and cons of existing impedance instrumentation methods. Section IV analyzes the frequency response of the tBLM model and introduces a new method to achieve high-resolution real-time tBLM characterization. The summary statements in Section V serve as guidelines for realizing real-time EIS.

II. tBLM Model

The tBLM structure shown in Fig. 1 consists of a lipid bilayer membrane with embedded proteins attached to a gold electrode using tethering lipids between spacer molecules[13]. The impedance of the interface is measured between the electrode and the solution outside of the membrane, with the physical components of the system corresponding to impedance elements in a tBLM equivalent circuit model. Electricity flows through the solution by the movement of ions in the solution, and the resistance to ion movement in the outside solution is modeled by R_s. The membrane acts as an insulator and thus creates a capacitance, C_m, between the outside solution and the solution below the membrane. The proteins allow limited ion flow between the two solutions and thus create a resistance, R_m, in parallel with the membrane capacitance. Within the solution, ions are the primary mode of conduction. However ions can not flow into the gold electrode; they can only create a charge at the surface of the electrode. The charge buildup at this solution-metal boundary is known as the double layer capacitance, C_{dl}. Typical values and ranges for these tBLM model parameters are shown in Table I. The total impedance Z for the tBLM equivalent circuit can be written as

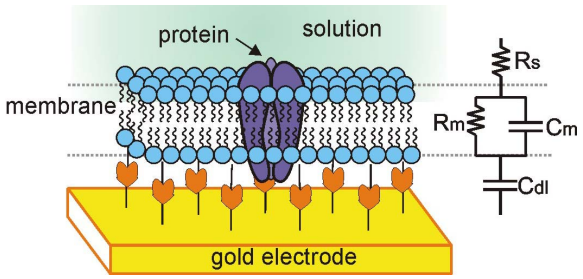

Fig. 1. The components of the equivalent circuit map directly to the physical structure of the sensor.

$$Z(\omega) = \frac{1 - C_{dl}C_m R_m R_s \omega^2 + j(C_m R_m + C_{dl} R_m + C_{dl} R_s)\omega}{-C_{dl}C_m R_m \omega^2 + jC_{dl}\omega} \quad (1)$$

where ω is the angular frequency.

The membrane protein sensor response is primarily within the R_m component of the tBLM interface impedance. For example, when an ion channel proteins open in response to specific analytes, ions are allowed to flow through the interface, reducing value of R_m. Thus, to characterize membrane protein activity, ΔR_m is the primary parameter of interest and all others can be ignored, if possible.

III. Analysis of tBLM Impedance Measurement

To perform EIS measurements, the two primary instrumentation approaches are frequency response analysis (FRA) and fast Fourier transform (FFT). In FRA, a small amplitude (10mV) sinusoid voltage stimulus is applied between the two biosensor electrodes, and the current response is measured as the frequency of the stimulus voltage is swept. Because FRA makes multiple measurements at successive frequencies, it is inherently slow for low frequency measurements. In contrast, FFT applies a broadband stimulus, typically a step voltage, and digitizes the response current for a length of time proportional to the desired frequency content. The digital results are then processed using Fourier transforms to extract the frequency components of the response and generate an impedance spectrum. Both approaches have been implemented in miniaturized instrumentation systems utilizing CMOS microelectronics, with FFT utilizing digital circuits [12] while FRA employs analog circuits [14, 15].

The time required to record an impedance spectrum varies greatly with the desired frequency range. Biosensors typically show impedance properties within a low frequency spectrum, 1mHz – 10kHz, while tBLMs are often measured at the low end of that range. Although FFT is generally faster that FRA for measuring the full impedance spectrum, the nature of FFT requires a much larger dynamic range and higher accuracy for measurements spanning multiple decades. Furthermore, for sensor arrays with up to hundreds of elements, FFT requires massive amounts of memory and a high-resolution ADC, which are very costly in terms of circuit area and power consumption [16].

TABLE I
TYPICAL VALUE OF TBLM MODEL PARAMETERS

	Min.	Typical	Max.
R_m	100kΩcm²	5MΩcm²	10MΩcm²
C_m	100nF/cm²	700nF/cm²	1.5μF/cm²
C_{dl}	5μF/cm²	5μF/cm²	5μF/cm²
R_s	50Ω	50Ω	50Ω
Area	0.25mm²	1mm²	1mm²

In sensor applications of membrane proteins, changes in R_m is typically the only parameter that needs to be monitored [10, 14]. For example, when ion channels open and close, that activity reflects directly in the R_m parameter and the other parameters can be ignored. Observing changes in R_m can be achieved by measuring tBLM impedance at a single frequency rather than scanning a broad frequency spectrum, with added advantages of increased readout speed and reduced instrumentation hardware complexity compared to traditional EIS. Using traditional approaches, R_m is typically calculated from impedance magnitude data taken below 100Hz because the impedance is dominated by other parameters at higher frequencies. However this is not fast enough for real-time measurement or observation of single channel activity that occurs in the kHz range, and a new approach capable of measuring changes in R_m with millisecond resolution is needed.

To illustrate the limitation of the impedance magnitude extraction approach, the frequency spectrum of the tBLM model in Fig. 1 was carefully analyzed. Fig. 2 shows the tBLM model impedance spectrum in the frequency range from 0.1mHz to 100MHz using the typical values in Table I. To represent a change of R_m, a second spectrum is plotted in a dash line after increasing R_m by a factor of three. Analysis of the tBLM equivalent electrical model reveals several important features of the impedance magnitude: 1) C_{dl} is the dominate element at low frequencies, 2) R_s dominates at high frequencies, 3) C_m is the dominate element at a mid-range frequencies when $\omega > 1/R_m C_m$, and 4) R_m is the dominate element at a mid-range frequencies when $\omega < 1/R_m C_m$. These regions are indicated at the top of Fig. 2, which reveals that changes in R_m are only observable in the impedance response magnitude at frequencies where R_m is

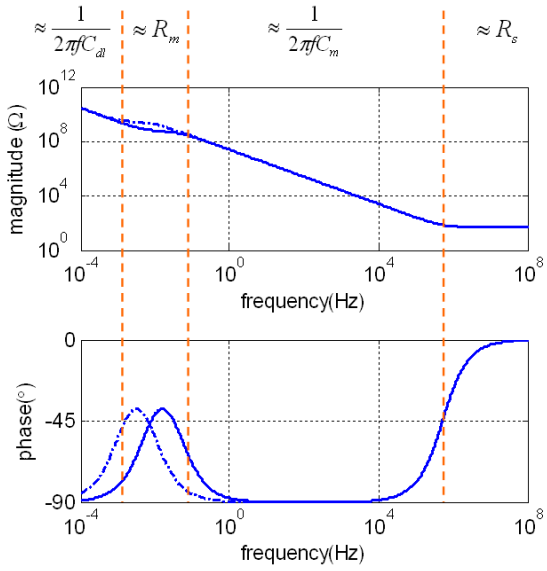

Fig. 2. Impedance spectrum of a tBLM from 0.1mHz to 100MHz with typical values in Table I. The dash line represents tBLM model when R_m is increased by a factor of three.

dominant. For typical tBLM model values, the "sweet spot" for measuring R_m is around 10mHz. However, at this frequency, even a single measurement of a full sinusoid stimulus period would take 100sec, which is too slow for real-time readout and precludes measurement of millisecond protein activity. At higher frequencies where C_m is dominant, even significant changes in R_m produce indistinguishable changes in the impedance magnitude.

IV. New Approach for tBLM Impedance Measurement

To identify a means by which changes in R_m can be measured at a higher frequency, notice that impedance can also be expressed in terms of real and imaginary components. Although the imaginary portion is dominated by C_{dl} and C_m, the real portion merits further investigation[9]. The following discussion is in terms of admittance, the reciprocal of impedance because many FRA instrumentation circuits can more easily extract admittance than impedance[14, 15]. From (1), the real portion of admittance Y can be written as

$$\mathrm{Re}(Y)=\frac{\omega^2+\frac{1}{R_m R_s C_m^{\,2}}+\frac{1}{R_m^{\,2} C_m^{\,2}}}{\frac{1}{C_{dl}^{\,2} C_m^{\,2} R_m^{\,2} R_s}\frac{1}{\omega^2}+R_s\omega^2+\frac{1}{R_s C_m^{\,2}}(1+\frac{C_m}{C_{dl}})^2} \quad (2)$$

Noticing that $R_m >> R_s$, the third term in numerator can be omitted as in following derivations.

Fig. 3 plots Re(Y) using typical values in Table I along with a second plot (dashed) with R_m three times higher than the typical value. The real admittance response can be divided into four frequency regions with distinct patterns as indicated in Fig. 3. Changing R_m causes an obvious variation in Re(Y) in regions (1) and (2), which are between 0.1mHz and 100Hz for typical model values. Compared to the magnitude plot in Fig. 2, R_m dominates Re(Y) over a much wider frequency range. The role of R_m in each region can be more clearly described by the simplified mathematical expression for Re(Y) within each region.

Region (1) is defined by $\omega < 1/R_m C_{dl}$. Here, Re(Y) can be simplified to

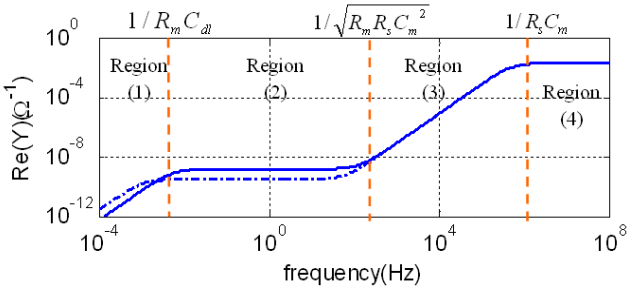

Fig. 3. Real portion of tBLM admittance with typical tBLM model values from 0.1 mHz to 100MHz. The dashed line represents an increase in R_m by a factor of three.

$$\mathrm{Re}(Y)_1 = C_{dl}^{\,2} R_m \omega^2 \quad (3)$$

which shows that Re(Y) is proportional to R_m at a given frequency. Region (2) is defined by $1/R_m C_{dl} < \omega < 1/\sqrt{R_m R_s C_m^{\,2}}$, where Re($Y$) can be simplified to

$$\mathrm{Re}(Y)_2 = \frac{1}{R_m}\frac{1}{(1+\frac{C_m}{C_{dl}})^2} \quad (4)$$

which shows that Re(Y) is proportional to $1/R_m$. Region (3) is defined by $1/\sqrt{R_m R_s C_m^{\,2}} < \omega < 1/R_s C_m$, where Re($Y$) can be simplified as

$$\mathrm{Re}(Y)_3 = \frac{\omega^2+\frac{1}{R_m}}{(1+\frac{C_m}{C_{dl}})^2} \quad (5)$$

which shows that the significance of R_m decreases as frequency increases. Finally, Region (4) is defined by $\omega > 1/R_s C_m$, where Re(Y) can be simplified to

$$\mathrm{Re}(Y)_4 = \frac{1}{R_s} \quad (6)$$

which is not a function of R_m. (3) – (6) verify the observation from Fig. 3 that R_m plays a dominate role only in Regions (1) and (2). The highest frequency at which R_m could be expected to provide a significant response in Re(Y) is defined by f_{ub2}, the up boundary of Region (2)

$$f_{ub2} = 1/\sqrt{R_m R_s C_m^{\,2}} \quad (7)$$

At all frequencies lower than f_{ub2}, the gain, G, of normalized Re(Y) with respect to normalized R_m,

$$G = \frac{\Delta \mathrm{Re}(Y)/\mathrm{Re}(Y)}{\Delta R_m / R_m} \quad (8)$$

is equal to 1 when ΔR_m is small.

To illustrate the potential benefit of the Re(Y) approach in terms of measurement speed, Fig. 4 plots the normalized gain over frequency in response to 10% change in R_m[10]. For comparison, the real, imaginary and magnitude components are shown using typical tBLM model parameter values. Notice that the gain drops significantly below 1 for imaginary and magnitude components at frequencies above 10mHz, making rapid measurements of ΔR_m impossible with any reasonable resolution. In contrast, the real component maintains a gain of nearly 1 up to 144Hz and thus can provide high resolution measurement of ΔR_m at much faster speeds.

Variations in tBLM model parameter values have a significant effect on f_{ub2}, which defines the maximum frequency to observe ΔR_m with high resolution. Table II shows the values of f_{ub2} from (7) using different model

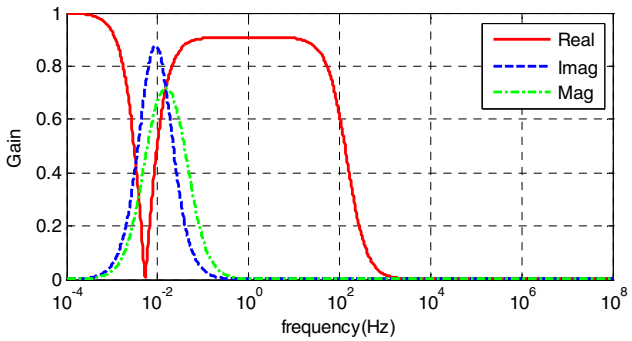

Fig. 4. Gain comparison of real, imaginary and magnitude components of admittance change in response to 10% change of R_m as a function of frequency.

TABLE II.
VARIATION IN MAXIMUM FREQUENCY FOR R_M MEASUREMENT WITH TBLM MODEL PARAMETER VALUES

tBLM Model Parameters	f_{ub2} (Hz)
Min	14,000
Typical	144
Max	47

parameter values from Table I. The best case permits 14kHz measurement, indicating that the millisecond behavior of membrane protein activity can be observed using impedance methods with a single point measurement at a high frequency. In practice, the values of R_m and C_m are hard to control during tBLM fabrication. However, observing that R_m is inversely proportional to area and that C_m is proportional to area, f_{ub2} is indirectly proportional to the square root of area

$$f_{ub2} \propto 1/\sqrt{area} \qquad (7)$$

Thus using a small tBLM area ($0.25mm^2$) will help to maximize f_{ub2} to enable high frequency measurements.

V. CONCLUSION

Membrane proteins have great potential in sensor applications and can be immobilized on electrodes using tBLMs. However, characterization using traditional impedance measurements has inherent limitations in terms of measurement speed. This paper has analyzed the electrical impedance model of tBLM containing membrane proteins and demonstrated that measurement of the real portion of admittance is an effective method for maximizing measurement speed. Changes in membrane resistance can be observed in the real portion of admittance at higher frequency than in imaginary or magnitude components. The maximum measurement frequency for high resolution measurement is a function of tBLM model parameters, and minimizing tBLM area was shown to increase the maximum measurement frequency. The best case permits measurements at 14kHz, enabling real-time readout of single channel activity with millisecond behavior

ACKNOWLEDGMENT

This work was supported in part by National Science Foundation (NSF) Award Number DBI-0649847 and the NSF Engineering Research Centers Program under Award Number EEC-9986866.

REFERENCES

[1] A. L. a. D. J. C. a. S. Mullner, "Protein biochips: A new and versatile platform technology for molecular medicine," *Drug Discovery Today*, vol. 10, pp. 789-794, 2005.

[2] A. J. Mason and H. Yue, "Membrane protein biosensor arrays on CMOS," *Asia Symposium on Quality Electronic Design (ASQED)* pp. 212-218, 2010.

[3] E. Katz and I. Willner, "Probing Biomolecular Interactions at Conductive and Semiconductive Surfaces by Impedance Spectroscopy: Routes to Impedimetric Immunosensors, DNA-Sensors, and Enzyme Biosensors," *Electroanalysis*, vol. 15, pp. 913-947, 2003.

[4] J.-G. Guan, Y.-Q. Miao, and Q.-J. Zhang, "Impedimetric biosensors," *Journal of Bioscience and Bioengineering*, vol. 97, pp. 219-226, 2004.

[5] J. S. Daniels and N. Pourmand, "Label-Free Impedance Biosensors: Opportunities and Challenges," *Electroanalysis*, vol. 19, pp. 1239-1257, 2007.

[6] B.-Y. Chang and S.-M. Park, "Electrochemical Impedance Spectroscopy," *Annual Review of Analytical Chemistry*, vol. 3, pp. 207-229, 2010.

[7] W. Knoll, I. Koper, R. Naumann, and E.-K. Sinner, "Tethered bimolecular lipid membranes--A novel model membrane platform," *Electrochimica Acta*, vol. 53, pp. 6680-6689, 2008.

[8] A. Offenhäusser, R. Rinaldi, I. Köper, I. K. Vockenroth, and W. Knoll, "Ion Channels in Tethered Bilayer Lipid Membranes on Au Electrodes," in *Nanobioelectronics - for Electronics, Biology, and Medicine*, *Nanostructure Science and Technology*, D. J. Lockwood, Ed.: Springer New York, 2009, pp. 211-223.

[9] A. Manickam, A. Chevalier, M. McDermott, A. D. Ellington, and A. Hassibi, "A CMOS Electrochemical Impedance Spectroscopy (EIS) Biosensor Array," *IEEE Transactions on Biomedical Circuits and Systems*, vol. 4, pp. 379-390, 2010.

[10] Y. Temiz, F. K. Gurkaynak, S. Terrettaz, H. Vogel, G. De Micheli, Y. Leblebici, C. Guiducci, and L. Benini, "Real-time high-sensitivity impedance measurement interface for tethered BLM biosensor arrays," *IEEE Int. Conf. on Sensors*, pp. 650-653, 2008.

[11] A. L. Ghindilis, M. W. Smith, K. R. Schwarzkopf, C. Zhan, D. R. Evans, A. M. Baptista, and H. M. Simon, "Sensor Array: Impedimetric Label-Free Sensing of DNA Hybridization in Real Time for Rapid, PCR-Based Detection of Microorganisms," *Electroanalysis*, vol. 21, pp. 1459-1468, 2009.

[12] D. S. Messing, A. Ghindilis, and K. Schwarzkopf, "Impedimetric biosignal analysis and quantification in a real-time biosensor system," *IEEE Int. Conf. on Engineering in Medicine and Biology Society (EMBC)*, pp. 2730-2734, 2010.

[13] B. A. Cornell, V. L. B. Braach-Maksvytis, L. G. King, P. D. J. Osman, B. Raguse, L. Wieczorek, and R. J. Pace, "A biosensor that uses ion-channel switches," *Nature*, vol. 387, pp. 580-583, 1997.

[14] Y. Chao, S. R. Jadhav, R. M. Worden, and A. J. Mason, "Compact Low-Power Impedance-to-Digital Converter for Sensor Array Microsystems," *IEEE Journal of Solid-State Circuits*, vol. 44, pp. 2844-2855, 2009.

[15] L. Xiaowen, D. Rairigh, and A. Mason, "A fully integrated multi-channel impedance extraction circuit for biosensor arrays," *IEEE Int. Symp. Circuits and Systems (ISCAS)*, pp. 3140-3143, 2010.

[16] D. Rairigh, A. Mason, and C. Yang, "Analysis of On-Chip Impedance Spectroscopy Methodologies for Sensor Arrays," *Sensor Letters*, vol. 4, pp. 398-402, 2006.